# Density Dependence of Low-Frequency Edge Harmonic Oscillations in LHD H-Mode Plasmas

Wenqing HU<sup>1)\*</sup>, Tatsuya KOBAYASHI<sup>1,2,3)</sup>, Tokihiko TOKUZAWA<sup>1,2,3)</sup>

The Graduate University for Advanced Studies, SOKENDAI, Toki 509-5292, Japan
National Institute for Fusion Science, National Institutes of Natural Sciences, Toki 509-5292, Japan
Research Institute for Applied Mechanics, Kyushu University, Kasuga 816-8580, Japan

(Received 6 April 2025 / Accepted 25 June 2025)

This paper investigates the density dependence of low-frequency edge harmonic oscillations (LF-EHOs) in the Large Helical Device (LHD) H-mode plasmas. A series of discharges with varying density settings reveal that the L-H mode transition occurs above a certain density threshold, and LF-EHOs appear only above an even higher density threshold. In discharges exhibiting LF-EHOs, the cross-coherence between density and magnetic fluctuations for the fundamental frequency remains consistently high across the entire density range. In contrast, the cross-coherence for the second harmonic exhibits an increasing trend with higher plasma density. These findings suggest that the LF-EHO potentially plays a noticeable role in edge profile saturation.

© 2025 The Japan Society of Plasma Science and Nuclear Fusion Research

Keywords: LHD, H-mode, MHD fluctuation, L-H mode transition, beam emission spectroscopy (BES)

DOI: 10.1585/pfr.20.1402044

#### 1. Introduction

The L-H mode transition is a well-known phenomenon in magnetically confined fusion plasmas, leading to improved confinement of plasma density, temperature, and pressure [1]. In tokamaks, a particular H-mode regime called the quiescent H-mode (QH-mode) offers improved confinement without the detrimental edge-localized modes (ELMs) [2]. In QH-mode, particle transport is believed to be driven by a continuous magnetohydrodynamic (MHD) instability known as the edge harmonic oscillation (EHO) [3, 4]. First discovered in tokamak plasmas, the same phenomena regarding L-H mode transition have also been confirmed in the other stellarators such as TJ-II [5], W7-AS [6, 7] and LHD [8, 9]. The characteristics for the L-H mode transition in stellarators are similar to those in tokamaks, namely, the spontaneous drop of H<sub>a</sub> at the transition, the improvement of the confinement, and the high gradient at the edge region.

In the Large Helical Device (LHD), a helical stellarator, an ELM-less L-H mode transition is observed where density confinement improves without a corresponding improvement in temperature confinement [10]. Low-frequency harmonic fluctuations, termed low-frequency edge harmonic oscillations (LF-EHOs) due to their lower fundamental frequency compared to tokamak EHOs, appear after this transition and are accompanied by magnetic fluctuations. Previous studies have shown that while density and magnetic fluctuations exhibit high coherence at the fundamental frequency of LF-EHOs,

their coherence at higher harmonics is significantly lower [10].

Previous investigations of the EHO that appears in the CHS stellarator during the QH-mode periods suggest that the appearance of EHO is involved with the saturation of the density gradient [11]. Subsequently, a more thorough analysis was conducted with the BES measurement and further clarified the spatial structure of the harmonic oscillation [12, 13]. In order to discuss the characteristics of the LF-EHOs despite the limited measurement locations of BES, a discussion with the cross-correlation between the plasma density and the electric/magnetic field is necessary. This kind of prospective has yet to be tried in the LHD previously.

This paper aims to investigate the density dependence of LF-EHO characteristics. Specifically, we analyze a series of LHD discharges with varying density settings to examine the density thresholds for the L-H mode transition and the appearance of LF-EHOs. We then explore the density dependence of the cross-coherence between density and magnetic fluctuations.

# 2. Experimental Setup and Target Discharge

The experiments were conducted in the LHD, a large superconducting helical device with a major radius of 3.9 m and an average minor radius of 0.6 m [14]. The discharges analyzed in this study employed a magnetic field strength of 1 T counter-clockwise and a magnetic axis position of 3.6 m. The plasma was primarily heated by neutral beam injections (NBIs) with a total port through power of about 10 MW.

The primary diagnostics used in this study are the beam emission spectroscopy (BES) system [15] and the magnetic

<sup>\*</sup>Corresponding author's e-mail: hu.wenqing@nifs.ac.jp

probe array [16]. The BES system measures local electron density fluctuations by analyzing the Doppler-shifted H<sub>a</sub> emission from a diagnostic neutral beam (NBI#3). The system consists of an 16 × 16 array of optical fibers coupled to avalanche photodiodes (APDs) with 8 × 8 pixels, providing a spatial resolution of approximately 4 cm and a temporal resolution of 5 µs. The magnetic probe array, installed inside the vacuum vessel, measures magnetic field fluctuations. Figure 1 shows spectrograms of the density fluctuations measured by BES at  $r_{\rm eff}/a_{99} = 0.85$  and the magnetic fluctuations measured by a magnetic probe. The horizontal axis represents time in seconds, and the vertical axis represents frequency in kilohertz. The spectrograms clearly demonstrate that the density fluctuations appear simultaneously with the magnetic fluctuations after the L-H mode transition. Both fluctuations are continuously present, a key feature distinguishing them from ELMs. The poloidal structure of the LF-EHO is analyzed using the poloidal channel array of the BES, which reveals a poloidal mode number of m = 1 for the fundamental mode and m = 2 for the second mode. Similarly, the toroidal mode number is obtained from the coherence analysis of the magnetic probe toroidal array signals. The toroidal mode numbers are n = 2 and n = 4 for the fundamental and second modes, respectively. Further more, the location where  $\iota/2\pi = 2$  is outside the  $\rho = 1$  border. Therefore, the modes are considered to be driven by the edge density gradient that peaks around the n/m = 2/1 rational surface at the plasma periphery. The mode amplitude was confirmed to peak at the outermost channel of BES [15].

# 3. Density Dependence of L-H Transition and LF-EHO Occurrence

To investigate the density dependence of the L-H transition and LF-EHOs, a series of discharges were performed with varying density settings while keeping other parameters constant. Three distinct scenarios were observed, as illustrated in Fig. 2:

- 1. Low Density: No L-H transition, no LF-EHOs after reaching the target density.
- Intermediate Density: L-H transition occurs after reaching the target density, but no LF-EHOs are observed.
- High Density: L-H transition occurs before reaching the target density, followed by the appearance of LF-EHOs.

In Fig. 2, the horizontal axes show zoomed-in time ranges around the point where the density reaches the target value or an L-H transition occurs. The top row shows the line-averaged electron density ( $\bar{n}_{\rm e}$ ), and the bottom row shows the H<sub>a</sub> emission intensity. The gray lines indicate the gas puff input used to control the density. This plot also demonstrates that the intensity of the gas puff decreases when the density reaches the set value for each discharges due to the feedback control scheme. In LHD, a spontaneous drop in H<sub>a</sub> emission during the density ramp-up is considered a useful indicator

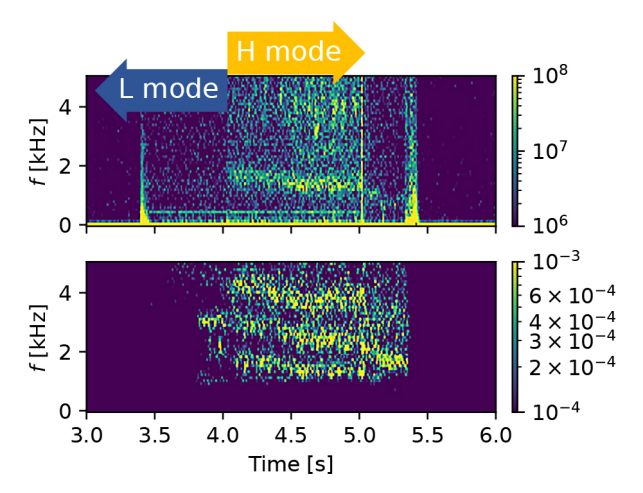


Fig. 1. Time evolution of spectra for (top) the density fluctuations measured by BES and (bottom) the magnetic fluctuations measured by a magnetic probe.

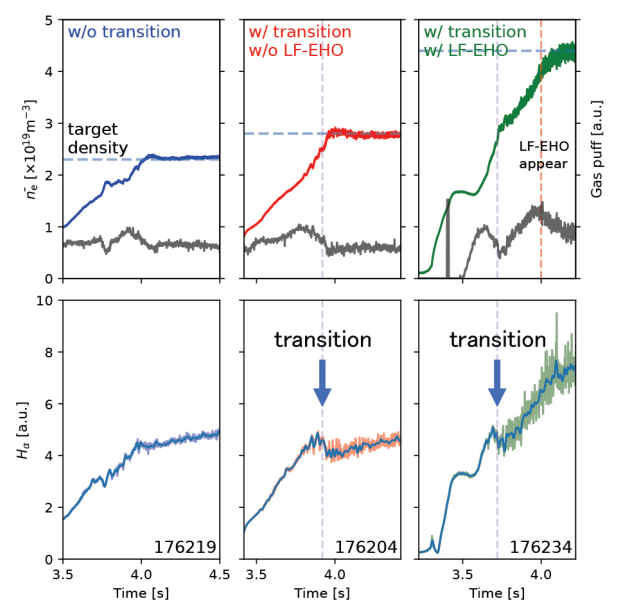


Fig. 2. Examples of the three discharge scenarios observed when varying the density setting. Left column: without LF-EHOs and without an L-H mode transition; center column: with an L-H mode transition but without LF-EHOs; right column: with an L-H mode transition and with LF-EHOs. Horizontal dashed lines indicate the target setting of the density feedback control.

of an L-H transition. The left column shows a case where the density is too low for either an L-H transition or LF-EHOs to occur. The density reaches the target value and stabilizes. The center column shows a case with a higher density setting, where an L-H transition occurs but no LF-EHOs are observed. The right column shows a case with an even higher density setting. In this discharge, the L-H transition occurs during the density ramp-up. Interestingly, LF-EHOs appear only after a further increase in density, not immediately after the L-H transition. Here, the appearance of LF-EHO is judged by the spectrum of the magnetic probe signal, where a continuous mode with high harmonics is clearly visible, which is demonstrated with the discharge shown in Fig. 1. The same

phenomena can be distinguished in EHOs for both tokamaks [4, 17] and stellarators [9, 11, 12]. This suggests that the appearance of LF-EHOs requires a higher density threshold than the L-H transition.

Figure 3 presents the power and density characteristics of the discharges in our experiment. The horizontal axis represents the density, and the vertical axis represents the port through total NBI heating power. The plotted trajectories represent the stable periods of each discharge, color-coded according to the occurrence of an L-H transition and/or LF-EHOs. For example, in the case of #176234 (shown in Fig. 2 right most column), a transient period 3.7 < t < 4.1 s is excluded. The power region below 9 MW is unintentional, resulting from NBI breakdowns. The absence of the L-H transition in discharge #176235, despite high-density conditions similar to discharge #176226 (which did transition), can be attributed to the timing of an NBI system breakdown: in #176235, the breakdown occurred before the transition could happen, while in #176226, it happened after the mode transition. The overlap of L-mode/H-mode points for #176234/ #176226 can be therefore attributed to the hysteresis in the H-mode transition condition. In our experiment, the density thresholds for the L-H transition and the appearance of LF-EHOs were approximately  $2.5 \times 10^{19}$  m<sup>-3</sup> and  $3.3 \times 10^{19}$  m<sup>-3</sup>, respectively.

# 4. Density Dependence of Cross-Coherence

The cross-coherence between density fluctuations (measured by BES) and magnetic fluctuations (measured by magnetic probes) was analyzed for discharges with varying densities. The same BES and magnetic probe channel is

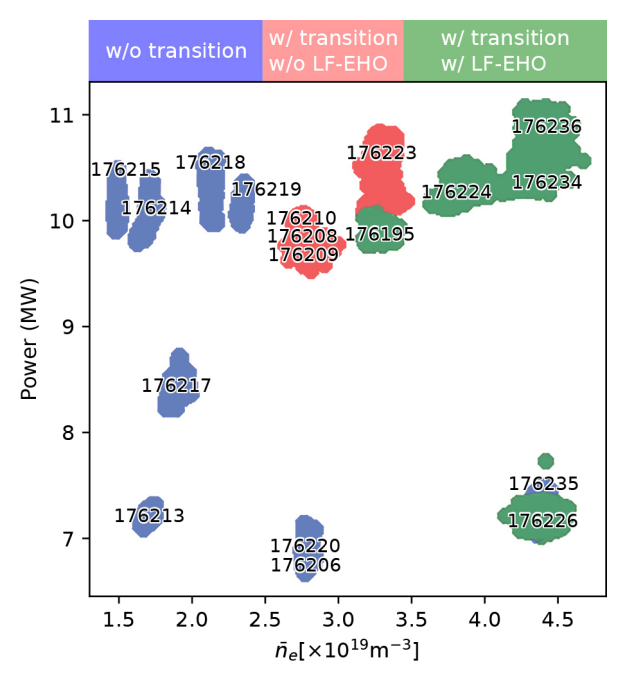


Fig. 3. Density and power trajectories for the three discharge scenarios, categorized by the presence or absence of an L-H mode transition and LF-EHOs.

chosen for each discharge to be analyzed. Six discharges with LF-EHOs are analyzed here. Figure 4 shows the squared cross-coherence,  $\gamma^2$ , as a function of frequency for different density settings. The horizontal axis represents frequency, and the subplots are arranged in order of ascending density. The fundamental harmonic of the LF-EHOs exhibits consistently high coherence across the entire density range. In contrast, the coherence of the second harmonic increases with density.

Next, the density dependence of the cross-coherence of the second harmonic is quantified. Figure 4 also reveals that the peak frequency of the LF-EHOs varies with density. The discrete Fourier transform used in the coherence analysis does not provide adequate frequency resolution to precisely locate the second harmonic peak, especially when the coherence is low. Weighted average frequency,  $\bar{f}$ , was calculated for the fundamental harmonic peak using the following formula:

$$\bar{f} = \frac{\int_{f_p - \delta f}^{f_p + \delta f} \gamma^2(f') f' \, \mathrm{d}f'}{\int_{f_p - \delta f}^{f_p + \delta f} \gamma^2(f') \, \mathrm{d}f'},\tag{1}$$

where  $f_p$  is the initial estimate of the peak frequency,  $\gamma^2(f')$  is the squared cross-coherence, and the integration is performed over the frequency range from  $f_p - \delta f$  to  $f_p + \delta f$ , corresponding to the full width at half maximum (FWHM) of the fundamental peak, which is indicated in Fig. 4 as green vertical lines. The frequency of the second harmonic was then approximated as  $2\bar{f}$ . The calculated fundamental and second harmonic frequencies are represented as red vertical lines in the Fig. 4. The coherence value was taken from the discrete values with the closest frequency. Figure 5 replots the data from Fig. 4, showing the coherence values of the fundamental and second harmonics for each discharge. To

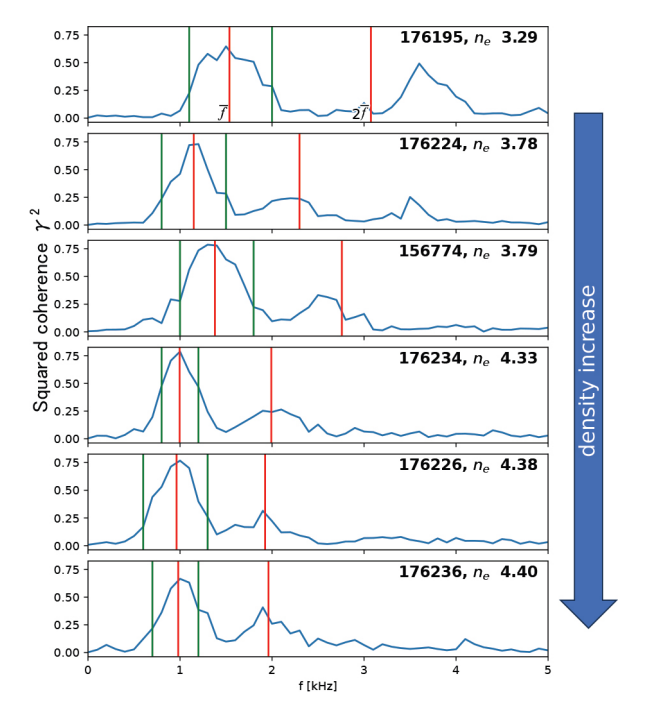


Fig. 4. Coherence between density and magnetic fluctuations for H-mode plasmas at different densities.

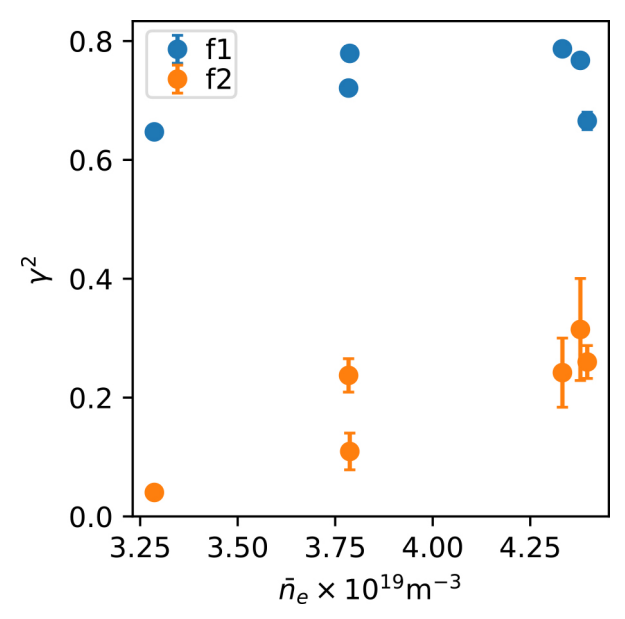


Fig. 5. Density dependence of the coherence between density and magnetic fluctuations for the fundamental (f1) and second harmonics (f2). The plotted values are the mean coherence calculated using an ensemble of six magnetic probe channels, and the error bars represent the standard error of the mean (SEM).

quantify the coherence and its statistical uncertainty, the cross-coherence was calculated between the density fluctuation signal from BES and the magnetic fluctuation signals from six toroidally separated magnetic probe channels. These six coherence values were treated as an independent ensemble for each discharge. The data points in the figure represent the mean of this ensemble, and the error bars indicate the standard error of the mean (SEM). The horizontal axis represents the average discharge density during the stable period, and the vertical axis represents the cross-coherence. The fundamental harmonic (blue dots) maintains consistently high coherence, while the coherence of the second harmonic (orange dots) increases with density, starting from low values at lower densities.

In addition to the coherence, the intensity of these harmonic signals provides further insight into their behavior. To investigate this aspect, Fig. 6 shows the density dependence of the fundamental and second harmonic signal intensity for BES and magnetic probe signals. The horizontal axis is the average plasma density of the stabilized H-mode period, and the vertical axis is the respective harmonic intensity normalized by the weakest signals. The fluctuation magnitude shown in the figures is proportional to the normalized BES intensity at the respective harmonic frequencies. In this figure, the harmonic intensities increase with density for both BES and magnetic probe signals. The sensitivity of the harmonic amplitude on the plasma density is higher than that of the fundamental mode amplitude, similar to the case of the coherence analysis. This tendency is more visible in the density fluctuation.

Furthermore, Fig. 7 presents the radial structure of the mode intensity for different density scenarios, plotted against major radius. This figure indicates that, in addition to the overall mode intensity being density dependent, the spatial

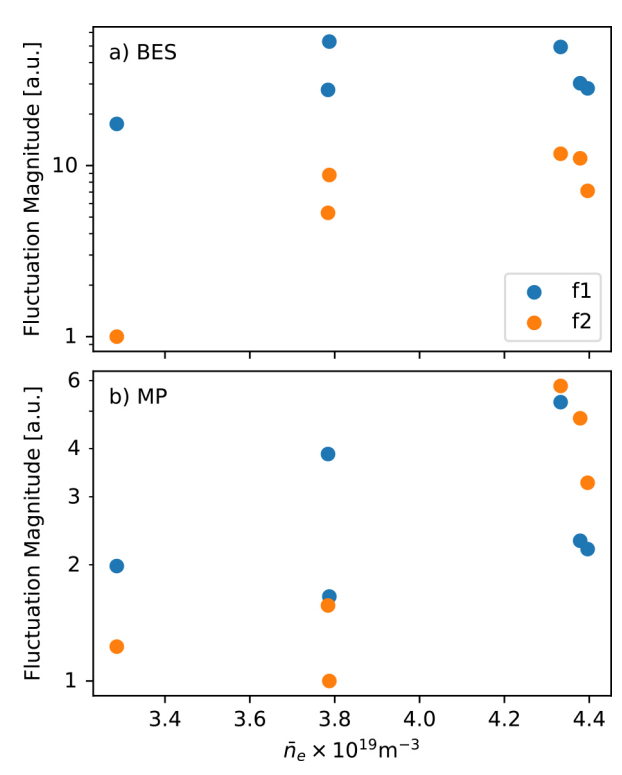


Fig. 6. Density dependence of the fundamental and second harmonic signal intensity for a) BES and b) magnetic probes.

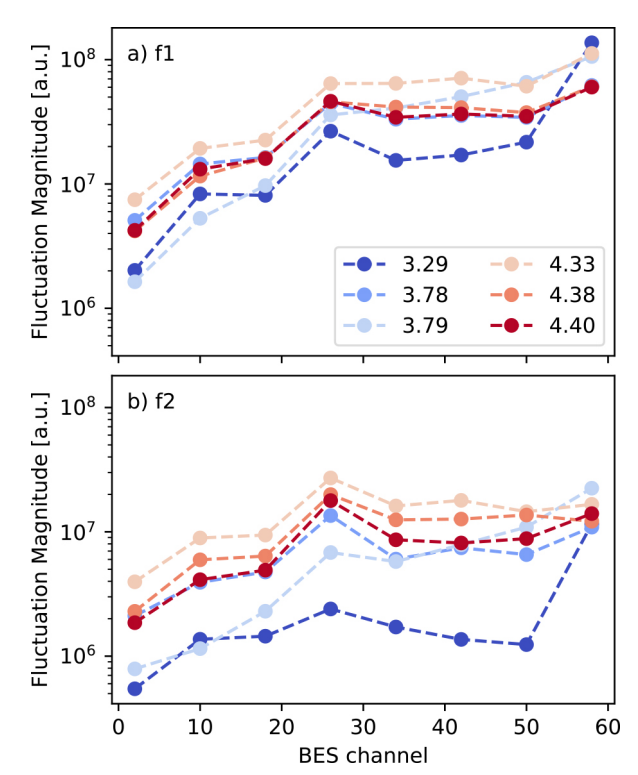


Fig. 7. Density dependence of the density fluctuation radial profile for the a) fundamental (f1) and b) second harmonics (f2).

structure of the harmonic modes also evolves as density increases. In particular, when the density is low, the LF-EHO is strong only at the outermost channel. While, as the density is increased, the radial extent of the LF-EHO is broadened into further inner radii.

### 5. Summary

In this research, the experimental results demonstrate that LF-EHOs in LHD H-mode plasmas exhibit a density dependence. They appear only above a certain density threshold, which is higher than the threshold for the L-H transition itself. By definition, cross coherence quantifies degrees of phase relation consistency between two fluctuating components of each frequency. The cross-coherence analysis reveals that while the fundamental harmonic of LF-EHOs maintains a consistent phase relationship between density and magnetic fluctuations across all densities, the second harmonic exhibits a density-dependent behavior. At lower densities, the second harmonic of density fluctuations has components that behaves independently of the magnetic surface, leading to low coherence. However, as the density increases, the phase relationship becomes more consistent, resulting in higher coherence.

The increasing coherence between density and magnetic fluctuations at higher densities can be interpreted that LF-EHOs, particularly their higher harmonics, play an increasingly important role in edge profile saturation as density increases. Although it is not a direct evidence, a finite coherence between the plasma density fluctuation and the magnetic fluctuation (likely correlated with the electric field) is a prerequisite for a finite fluctuation-driven transport. This density dependence is also reflected in the characteristics of the fluctuations themselves; both the intensities of the harmonic modes and the radial profile of the density fluctuation are found to be density dependent. The independent behavior of the second harmonic at lower densities might be related to different nonlinear evolution mechanisms, as suggested by the bicoherence and biphase analyses in our previous study [18].

In conclusion, this study discussed the density dependence of LF-EHO characteristics in LHD H-mode plasmas. The findings suggest that LF-EHOs can play a role in edge profile saturation, with their influence increasing at higher densities. Future work should focus on confirming these results with a larger dataset and exploring the underlying mechanisms responsible for the observed density dependence, potentially through detailed comparisons with simulations.

### Acknowledgments

The authors would like to thank Dr. Y. Suzuki, Dr. M. Yoshinuma, Dr. S. Sakakibara, Dr. K. Ogawa, Dr. K. Ida and LHD experiment group for their valuable contributions to earlier stages of this work, including insightful discussions and experimental support. Their efforts were instrumental in laying the groundwork for the present study. The authors also extend their gratitude to Prof. A. Fujisawa, Dr. M. Yokoyama, Dr. N. Kenmochi and Dr. T. Oishi for their support and guidance, as this work forms part of the first author's doctoral thesis.

The data supporting the findings of this study are available in the LHD experiment data repository [19]. This work was supported in part by the Collaborative Research Program of Research Institute for Applied Mechanics, Kyushu University.

- [1] F. Wagner et al., Phys. Rev. Lett. 49, 1408 (1982).
- [2] W. Suttrop et al., Plasma Phys. Control. Fusion 46, A151 (2004).
- [3] K.H. Burrell et al., Phys. Plasmas 23, 056103 (2016).
- [4] F. Wagner, Plasma Phys. Control. Fusion 49, B1 (2007).
- [5] T. Estrada et al., Contrib. Plasma Phys. 50, 501 (2010).
- [6] M. Hirsch et al., Plasma Phys. Control. Fusion 50, 053001 (2008).
- [7] K. McCormick et al., Phys. Rev. Lett. 89, 1 (2002).
- [8] K. Toi et al., Fusion Sci. Technol. 58, 61 (2010).
- [9] M. Ono et al., Plasma Fusion Res. 11, 1402115 (2016).
- [10] W. Hu et al., Plasma Fusion Res. 16, 2402031 (2021).
- [11] T. Oishi et al., Nucl. Fusion 46, 317 (2006).
- [12] S. Kado *et al.*, J. Nucl. Mater. **363-365**, 522 (2007), Plasma-Surface Interactions-17.
- [13] T. Oishi et al., Plasma Fusion Res. 3, S1010 (2008).
- [14] H. Takahashi et al., Nucl. Fusion 57, 086029 (2017).
- [15] T. Kobayashi et al., Plasma Phys. Control. Fusion 62, 13 (2020).
- [16] S. Sakakibara et al., Fusion Sci. Technol. 58, 471 (2010).
- [17] K.H. Burrell et al., Phys. Plasmas 8, 2153 (2001).
- [18] W. Hu et al., J. Phys. Soc. Jpn. 94, 064501 (2025), https://doi.org/ 10.7566/JPSJ.94.064501.
- [19] LHD experiment data repository, https://doi.org/10.57451/lhd. analyzed-data.